

AD-A096 070

LEHIGH UNIV BETHLEHEM PA MATERIALS RESEARCH CENTER

F/S 11/9

THE INFLUENCE OF ABSORBED MOISTURE ON FATIGUE CRACK PROPAGATION--ETC(U)

JAN 81 P E BRETZ, R W HERTZBERG, J A MANSON

N00014-77-C-0633

UNCLASSIFIED

TR-6

NL

1 OF 1
AD-A
1196070

END
DATE
FILMED
4-81
DTIC

(14) 711-6

LEVEL II

(12)

SECURITY CLASSIFICATION OF THIS PAGE (When Data Entered)

REPORT DOCUMENTATION PAGE		READ INSTRUCTIONS BEFORE COMPLETING FORM
1. REPORT NUMBER Technical Report #6	2. GOVT ACCESSION NO. AD A69607C	3. RECIPIENT'S CATALOG NUMBER C 1
4. TITLE (and Subtitle) The Influence of Absorbed Moisture on Fatigue Crack Propagation Behavior in Polyamides. Part B. Fractography.		5. TYPE OF REPORT & PERIOD COVERED Interim Technical Report
6. AUTHOR(s) Philip E. Bretz, Richard W. Hertzberg and John A. Manson		7. PERFORMING ORG. REPORT NUMBER N00014-77-C-0633
8. PERFORMING ORGANIZATION NAME AND ADDRESS Materials Research Center - Lehigh University Bethlehem, PA. 18015		9. PROGRAM ELEMENT, PROJECT, TASK AREA & WORK UNIT NUMBERS NR 356-670
10. CONTROLLING OFFICE NAME AND ADDRESS Office of Naval Research 800 N. Quincy Street Arlington, VA 22217		11. REPORT DATE January 1981
12. MONITORING AGENCY NAME & ADDRESS (if different from Controlling Office) 12/34		13. NUMBER OF PAGES 26
14. DISTRIBUTION STATEMENT (of this Report) Approved for public release; distribution unlimited.		15. SECURITY CLASS. (of this report) Unclassified
16. DISTRIBUTION STATEMENT (of the abstract entered in Block 20, if different from Report) Submitted to the Journal of Materials Science		17. SUPPLEMENTARY NOTES E
18. KEY WORDS (Continue on reverse side if necessary and identify by block number) Polyamides Fatigue Effects of Water Fatigue Crack Propagation Mechanisms of Failure Fractography Fracture		
19. ABSTRACT (Continue on reverse side if necessary and identify by block number) The fatigue fracture surface morphology of nylon 66, nylon 6 and nylon 612 was examined to ascertain mechanisms of fatigue crack propagation (FCP) in these polymers. Attention was also given to noting any correlation between fracture surface markings and macroscopic fatigue crack growth rate data. In general, observed changes in fracture surface appearance reflected an increasing level of plastic deformation with increasing water content, particularly in N66 and N6. Classical fatigue striations were identified in specimens of N66 and N6.		

DD FORM 1 JAN 73 1473

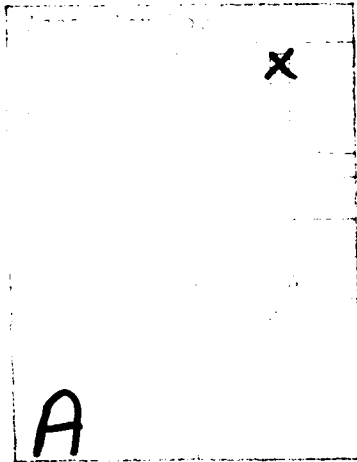
EDITION OF 1 NOV 65 IS OBSOLETE
S N 0102-014-6601408206
SECURITY CLASSIFICATION OF THIS PAGE (When Data Entered)

AD A69607C

DDC FILE COPY

20. ABSTRACT (continued)

containing 1.7-5.7 wt% water. Other types of fracture lineage of unknown origin were also seen which can confound the interpretation of fatigue fracture topography. Unlike the cases of N6 and N66, the fracture of N612 was dominated by a microvoid coalescence mechanism at all moisture levels and at all ΔK levels examined.



OFFICE OF NAVAL RESEARCH

Contract N00014-77-C-0633

Task No. NR 356-670

TECHNICAL REPORT NO. 6

THE INFLUENCE OF ABSORBED MOISTURE
ON FATIGUE CRACK PROPAGATION BEHAVIOR IN POLYAMIDES:
PART B - FRACTOGRAPHY

by

Philip E. Bretz, Richard W. Hertzberg and John A. Manson

Prepared for Publication
in the
Journal of Materials Science

Materials Research Center
Lehigh University
Bethlehem, Pa.
January 30, 1981

Reproduction in whole or in part is permitted for any purpose
of the United States Government.

This document has been approved for public release and sale;
its distribution is unlimited.

81 3 06 061

THE INFLUENCE OF ABSORBED MOISTURE
ON FATIGUE CRACK PROPAGATION BEHAVIOR IN POLYAMIDES:

PART B - FRACTOGRAPHY

by Philip E. Bretz,¹ Richard W. Hertzberg² and John A. Manson²

Abstract

The fatigue fracture surface morphology of nylon 66, nylon 6 and nylon 612 was examined to ascertain mechanisms of fatigue crack propagation (FCP) in these polymers. Attention was also given to noting any correlation between fracture surface markings and macroscopic fatigue crack growth rate data. In general, observed changes in fracture surface appearance reflected an increasing level of plastic deformation with increasing water content, particularly in N66 and N6. Classical fatigue striations were identified in specimens of N66 and N6 containing 1.7-5.7 wt% water. Other types of fracture lineage of unknown origin were also seen which can confound the interpretation of fatigue fracture topography. Unlike the cases of N6 and N66, the fracture of N612 was dominated by a microvoid coalescence mechanism at all moisture levels and at all ΔK levels examined.

¹Formerly Research Assistant, Lehigh University and currently Engineer, Alcoa Technical Center, Alcoa Center, PA 15069.

²Materials Research Center, Lehigh University, Bethlehem, PA 18015

The Influence of Absorbed Moisture
on Fatigue Crack Propagation Behavior in Polyamides:

Part B - Fractography

1. Introduction

In two earlier papers [1,2] and in Part A [3] of this investigation, the fatigue crack propagation (FCP) behavior of several polyamides (nylon 66, nylon 6 and nylon 612) was discussed. It was found that crack growth rates were a strong function of water content, particularly in nylon 66 and nylon 6, with propagation rates being a minimum at an intermediate moisture level (2-3 wt% H₂O). This growth rate minimum was concluded to reflect an optimum balance between moisture-enhanced blunting of the crack tip and lowering of the modulus in the bulk polymer. In the present paper, fracture surfaces of these three polyamides are examined and discussed in light of the observed variations in FCP behavior reported earlier [1-3].

One usually finds that the fracture surface morphology of a semi-crystalline polymer is more complex than that of an amorphous material, a fact which probably reflects the more complex multi-phase structures associated with semi-crystalline materials. Indeed, numerous studies [4-12] of fracture topographies in semi-crystalline polymer have described a variety of observations, many of which are without parallel in fractographic analyses of amorphous polymers. A recent study by the present investigators [13], however, does help to explain some of these fractographic features in terms of crack tip deformation processes. Nevertheless, the origin of many fractographic details in multi-phase polymers remains obscured.

To cite one example, the occurrence of parallel fracture surface markings oriented parallel to the crack front is often assumed, without

hesitation, to be evidence of crack growth by striation formation. While the term "striation," in a generic sense, can be applied to any set of lines, the term should more properly be reserved for those fracture markings whose spacing represents the incremental advance of the crack front resulting from one load excursion. Consequently, if only striations are found on the fracture surface, their spacing should correspond to the macroscopic crack growth rate. However, in several amorphous polymers [14,15] and in semi-crystalline polyacetal [15,16] and high-density polyethylene [11,12], a fracture lineage of fundamentally different origin has been identified. These so-called discontinuous growth (DG) bands represent sudden growth increments following 10^1 to 10^5 loading cycles where no crack extension occurred. Hence, the DG band spacing does not represent the cyclic crack velocity. Therefore, by comparing the spacing of a given set of fracture lines with the macroscopic growth rate, it is possible to determine whether the lines are striations or discontinuous growth bands.

The classification of fatigue fracture lineage in semi-crystalline polymers is further complicated by the fact that parallel fracture surface lines have been variously referred to as "striations," "microstriations," and "fatigue striations" [4-12]. For example, the "microstriations" in LDPE [6,7] were concluded to represent the ends of spherulite lamellae, with their spacing being equivalent to the lamellar thickness. This conclusion seems unlikely [17], however, since the reported lineage spacing ($\sim 1 \mu\text{m}$) is much larger than the typical lamellar thickness ($\sim 10 \text{ nm}$). It is clear, therefore, that the origin of any lineage on the fracture surfaces of semi-crystalline polymers must be very carefully determined by comparison of band widths with macroscopic growth rates and comparison with microstructural features.

The objective of this research was to identify and catalogue fatigue fracture surface details in several polyamides that had been equilibrated to various levels of absorbed moisture prior to testing. In light of the strong influence of moisture content on macroscopic fatigue crack growth rates in these polyamides [1-3], attention was given to noting any correlation between relative changes in FCP rates and in fracture topography as a function of moisture content.

2. Experimental Procedure

The fracture surfaces examined in this investigation corresponded to those polyamide samples which were used to generate crack propagation data as a function of moisture content [3]. These commercially-available grades of nylon included nylon 66 (N66) of two molecular weights (number-average molecular weights, M_n , of 17,000 and 34,000), nylon 6 (N6) ($M_n = 16,000$), and nylon 612 (N612). Specimens of these polymers had been equilibrated to various levels of absorbed moisture by vacuum drying or by boiling in various aqueous salt solutions, as described elsewhere [2,3], prior to fatigue testing.

The fracture surfaces were studied using an optical microscope and an ETEC Autoscan scanning electron microscope (SEM); for the latter instrument, a 20 kV accelerating voltage was used. Prior to SEM observation, specimens were prepared by either vacuum evaporation of gold and carbon or sputter-coating from a gold-palladium target. For several of the N612 specimens in which an energy-dispersive spectrum (EDS) analyzer was used as part of the examination, only carbon was evaporated onto the fracture surface.

Measurements of fatigue striation spacing were made on the moisture-equilibrated N66 and N6 specimens. Because these markings were seen on a part of the fracture surface in which the crack front was noticeably curved, it was necessary to correct crack length measurements for this curvature, using a procedure previously described [1].

3. Experimental Results and Discussion

3.1 Macroscopic Observations

Fractographic features of the various nylons are summarized in Tables 1-4, and it is clear that 1) stress whitening; 2) texture; and 3) the nature of terminal fracture, depend on water content. As has been discussed previously [1,2], the occurrence of stress whitening in nylon containing more than 1% water reflects the ability of these moisture-bearing samples to undergo significant plastic deformation, while the lack of stress whitening in dry samples indicates reduced plasticity.

The overall fracture surface texture of the specimens changes dramatically with moisture content. In the region of stable fatigue crack growth, the dry nylons develop relatively flat, featureless surfaces, as previously noted for N66 [1,2]; alternately, an increasingly rugged fracture surface topography is noted with increasing moisture content. In addition to the observations noted in Tables 1 through 4, N66 and N6 samples containing $\leq 5.7\%$ water exhibited coarse arrest lines parallel to the crack front at stress intensity levels above $3.7 \text{ MPa}\sqrt{\text{m}}$. Photographs of these markings for N66 ($MW = 17,000$) have been published in earlier papers (e.g., Fig. 3 in reference 1); these fractographs bear a similar appearance to those found in this study for N66 ($MW = 34,000$) and N6 (Fig. 1a). The markings, indicated by arrows, have been associated with the periodic interruption of the FCP test to read the crack tip position and imply the occurrence of creep. The finer lines between these arrest bands were found to be fatigue striations (see below).

During the actual fatigue tests, it was noted that the N66 specimens containing $\leq 4.5\%$ water failed by rapid, unstable crack propagation, whereas the specimens containing $\geq 4.5\%$ water failed by stable but very high growth rate ($> 1 \text{ mm/cycle}$) cyclic tearing at large ΔK levels. In the N6 tests, only dry specimens fractured in a brittle manner; on the other hand, all N612 specimens exhibited terminal fast fracture. As observed in previous

TABLE 1

Fractographic Observations - N66 (MW = 17,000)

	0% H ₂ O	0.8	2.2	2.6	2.8	4.0	4.5	5.7	8.5
Surface Whitening	No	No	Some	Some	Yes	Yes	Yes	Yes	Yes
Texture	Smooth	Smooth	Rough	Rough	Rough	Rough	Rough	Rough	Rough
Terminal Fracture	Brittle	Brittle	Brittle	Brittle	Brittle	Brittle	Tearing	Tearing	Tearing
Trans-spherulitic Failure	Yes	Yes	No	No	No	No	No	No	No
Striations	No	No	Yes	Yes	Yes	Yes	Yes	Yes	No
D.G. Bands @ 10 Hz	No	No	No	No	No	No	No	No	No

TABLE 2

Fractographic Observations - N66 (MW = 34,000)

	0% H ₂ O	1.7	2.6	8.5
Surface Whitening	No	Yes	Yes	Yes
Texture	Smooth	Rough	Rough	Rough
Terminal Fracture	Brittle	Brittle	Brittle	Tearing
Trans-spherulitic Failure	No	No	No	No
Striations	No	Yes	Yes	No
D.G. Bands @ 10 Hz	No	No	No	No

TABLE 3

Fractographic Observations - N6

	0% H ₂ O	2.5	2.7	8.5
Surface Whitening	No	Yes	Yes	Yes
Texture	Smooth	Smooth	Smooth	Rough
Terminal Fracture	Brittle	Tearing	Tearing	Tearing
Trans-spherulitic Failure	No	No	No	No
Striations	No	Yes	Yes	No
D.G. Bands	No	No	No	No

TABLE 4

Fractographic Observations - N612

	0% H ₂ O	1.1	3.2
Surface Whitening	No	No	Yes
Texture	Smooth	Smooth	Rough
Terminal Fracture	Brittle	Brittle	Brittle
Trans-spherulitic Failure	No	No	No
Striations	No	No	No
D.G. Bands	No	No	No



Fig. 1a



Fig. 1b

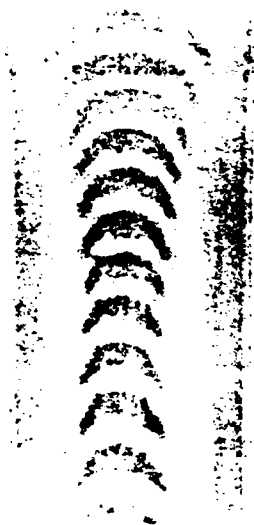


Fig. 1c

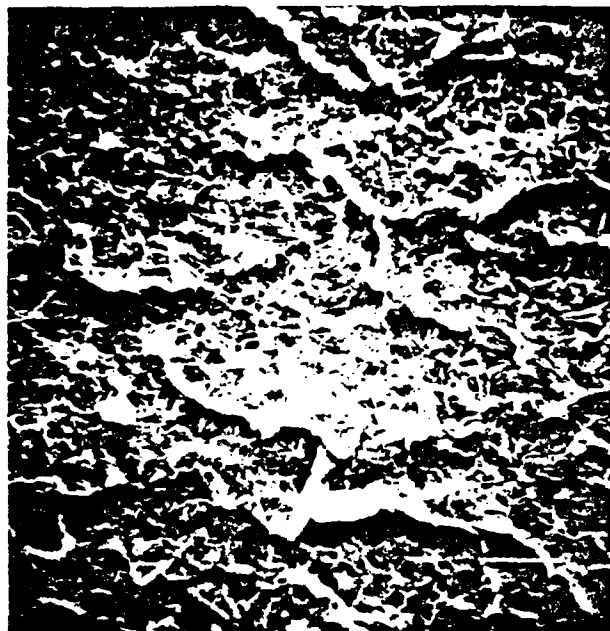
Figure 1 - Macroscopic fracture surface appearance in nylon 66. a) Coarse and fine arrest lines found on fatigue fracture surface in nylon 66 equilibrated to 50% r.h.; b) Fracture bands near back surface due to stress wave-crack front interactions; c) Widely spaced arrest lines believed to correspond to extent of tearing in each load cycle.

work (1), unstable crack propagation is accompanied by crack bifurcation in all cases, and is further characterized by the complete absence of stress whitening, regardless of moisture level. In addition, fracture bands from stress wave-crack front interactions are seen in the fast fracture regions of all nylon samples which failed by this mechanism (Fig. 1b). These bands are particularly notable, since they represent a type of fracture lineage which is clearly found in the fast fracture region and is in no way related to the fatigue process. The distinguishing feature noted on the terminal fracture surface regions of the N66 and N6 specimens which failed by tearing is the widely separated arrest lines believed to correspond to the extent of tearing in each load cycle (Fig. 1c).

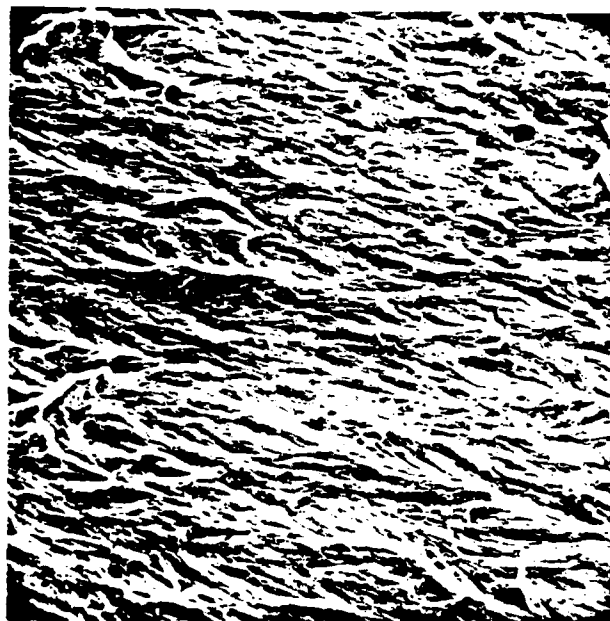
3.2 Microscopic Observation

As was the case with macroscopic observations, major differences were noted in the microscopic fracture surface morphology of nylon specimens equilibrated to different moisture levels. It was previously reported [1,2] that the fracture surface of dry N66 (MW=17,000) is patchy and shows evidence of trans-spherulitic fracture (Fig. 2a)*. A recent study of deformation mechanisms in semi-crystalline polymers [13] confirmed that trans-spherulitic fatigue fracture can occur when chain mobility is limited, thereby precluding significant plastic deformation at the crack tip. In contrast, the fracture surfaces of high-MW N66 specimens without water appeared drawn, though not to the extent of specimens of either type of N66 contained > 2% water (Fig. 2b). The absence of a trans-spherulitic fracture pattern in dry, high-MW N66 has been rationalized [18] in terms of a greater potential for withstanding cyclic damage prior to fracture in the high-MW polymer as compared to the low-MW nylon at the same ΔK level. This potential for deformation apparently causes the

*Crack propagation direction is from left to right in all electron fractographs unless marked otherwise.



(a)



(b)

Figure 2 Fracture surface morphology in dry N66.
 a) Patchy appearance ($M_n = 17,000$) $\Delta K = 2.1 \text{ MPa}\sqrt{\text{m}}$
 Scale bar = $30 \mu\text{m}$;
 b) Extensive drawing ($M_n = 34,000$) $\Delta K = 2.2 \text{ MPa}\sqrt{\text{m}}$
 Scale bar = $20 \mu\text{m}$.

spherulite structure at the fracture surface to be perturbed to such an extent that the spherulite morphology becomes unrecognizable.

In dry N6 specimens the fracture surface is somewhat reminiscent of a void coalescence mechanism (Fig. 3). These voids increase in size with ΔK , and at all stress intensity levels are much larger than the measured spherulite size of 8-10 μm ; therefore, the fracture mechanism in dry N6 does not appear to be structure sensitive. (The micromorphology of fatigue fracture in N612 will be discussed later, since the mechanism of fracture is noticeably different from that in N66 and N6.)

At higher moisture levels, the fracture surfaces of N66 and N6 samples were similar to one another but quite different from the topography of dry specimens. Figure 4 illustrates the extensive amount of plastic deformation evident on the fracture surfaces of both MW's of N66 and N6. The existence of the undulating bands on each of these fracture surfaces is quite striking and suggestive of fatigue striations, as the ridges and lineage are perpendicular to the crack growth direction. However, the size of these ridges is invariant over large regions of the fracture surface in which the crack growth rates change by an order of magnitude; furthermore, these ridges are at least several times larger than the macroscopic growth rates. Therefore, such lineage cannot be interpreted as being fatigue striations.

Frequently, a much finer set of lines perpendicular to the crack growth direction can be seen on the fracture surface, often near the larger ridges (Fig. 5). Again, however, the spacing of these lines precludes the possibility of their being fatigue striations. Teh and White [6,7] have interpreted similar markings in LDPE to be the edges of spherulite lamellae and the lineage spacing to be the lamellar thickness. However, the spacing of the fine lines in Fig. 5 is too large to permit this interpretation, since the lamellar thickness is expected to be about 100X smaller. Thus, while the origin

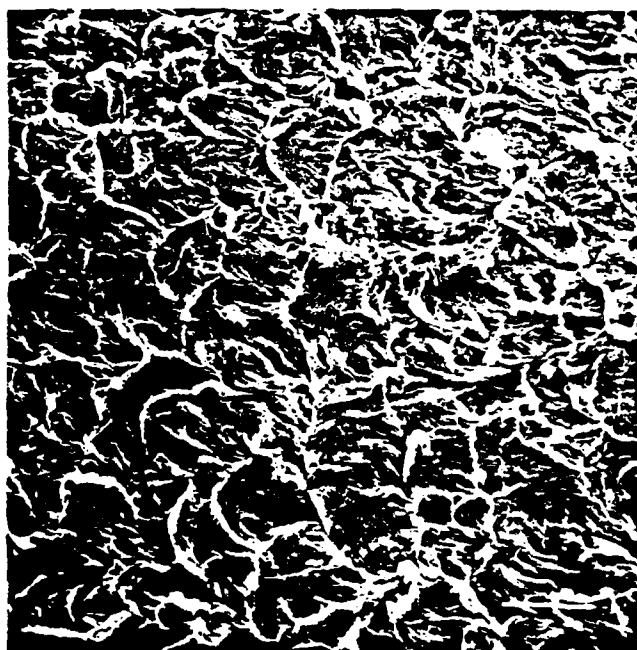


Figure 3 Patchy fracture morphology in dry N6,
reminiscent of a void coalescence mechanism.
Scale bar = 40 μm .



(a)



(b)



(c)

Figure 4 Evidence of severe crack tip plastic deformation.
a) N66 with 2.6% H_2O ($M_n = 17,000$). Scale bar = 20 μm ;
b) N66 with 2.6% H_2O ($M_n = 34,000$); c) N6 with 8.5% H_2O ,
Scale bar = 40 μm .



Figure 5 Fine lineage in N66 perpendicular to crack growth direction. Black arrows on micrograph indicate line spacing which does not correspond to macroscopic growth rate. White arrow indicates crack growth direction. Scale bar = 5 μ m.

of this complex lineage structure is unclear, it is apparent that extreme care must be exercised when interpreting the fracture surface details of semi-crystalline polymers.

A comparison of the fracture surface appearance in N66 as a function of MW is very interesting. As was noted previously, the fracture morphology of dry N66 was patchy in the low-MW material but noticeably drawn in the high-MW polymer (Fig. 2); also, crack growth rates in dry N66 were much lower in the high-MW material [3]. However, a comparison of the fracture appearance of water-containing N66 at different MW's (Figs. 4a and b) indicates little change in fracture mechanism with molecular weight. Significantly, there is also little effect of MW on crack growth rates in N66 containing $\geq 2.6\%$ H_2O [3]. Thus, there is a correlation between fracture appearance and crack growth rates.

The specimens of N66 containing intermediate moisture levels (1.5%-5.7% water) were the only nylons to support stable crack growth at stress intensity levels significantly greater than $4 \text{ MPa}/\text{m}$. Above this ΔK level, the fracture surface is covered with long, ribbon-like features oriented parallel to the direction of crack growth (Fig. 6). Interestingly, the width of these ribbons at their widest points is close to the bulk spherulite size. This correspondence in dimension is consistent with the observations of White and Teh [7], who found similar markings in LDPE and concluded that they represent the remnants of spherulites which had been drawn out in the direction of crack growth. As described by the authors elsewhere [13], spherulites at the crack tip are believed to be deformed by compressive stresses within the crack tip reversed plastic zone, which are oriented perpendicular to the crack plane. It is believed that such compressive yielding flattens and spreads the spherulites in the crack growth direction, and results in the formation of a series of

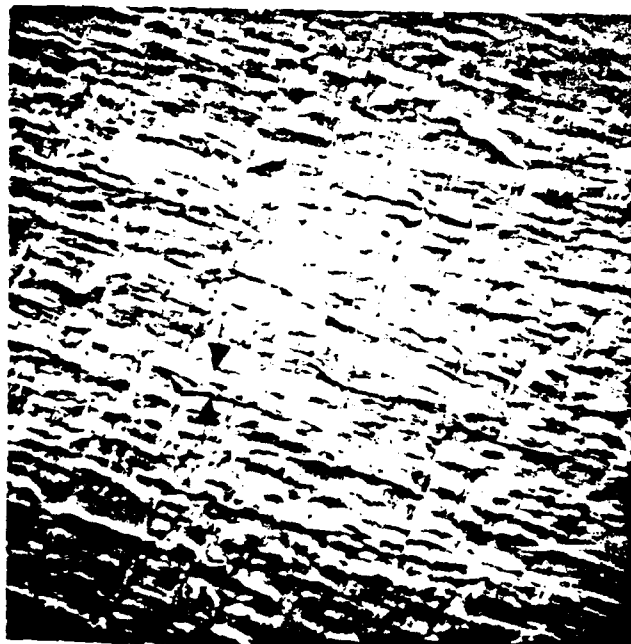


Figure 6 Ribbon-like features parallel to crack growth direction in N66 (2.2% H₂O). Arrows on micrograph indicate width of these ribbons, which are believed to be original diameter of deformed spherulites. $\Delta K = 5.7 \text{ MPa}\sqrt{\text{m}}$. Scale bar = 50 μm .

parallel lines with a spacing comparable to the original spherulite diameter (Fig. 6).

Classical fatigue striations were found on the fracture surfaces of N66 and N6 specimens containing intermediate levels of moisture (1.5-5.7%). The nature of these striations (e.g., Fig. 7) was verified by a comparison of their spacings with the corresponding macroscopic growth rates (Fig. 8). Because of the variety of fracture surface lineage observed in these semicrystalline polymers, such a comparison of macroscopic and microscopic growth rate data is essential to establish whether certain features are, indeed, fatigue striations.

No evidence of a discontinuous growth (DG) mechanism was seen on the fracture surfaces of any nylon fatigue specimen tested at 10 Hz, the standard test frequency for this program. However, DG markings were observed in specimens of N66 (both MW's) containing 2.6% water which were tested at 50 Hz [18]. Consequently, one must anticipate DG formation in service failures of structural polyamides under certain test conditions.

The fracture surfaces of the N612 samples are distinctive in that, regardless of moisture content, the mechanism of fatigue crack growth was microvoid coalescence (Fig. 9); no fracture lineage of any kind was observed on any specimen. The diameter of these microvoids increased linearly with ΔK (Fig. 10); interestingly, the voids in saturated N612 (3.2% H_2O) were noticeably larger than in the other specimens. The fact that these voids were largest in the N612 specimens which exhibited the lowest growth rates [3] is analogous to the observed relationship between toughness and microvoid size in metal alloys: void diameter and depth are found to increase with toughness in these materials [19].

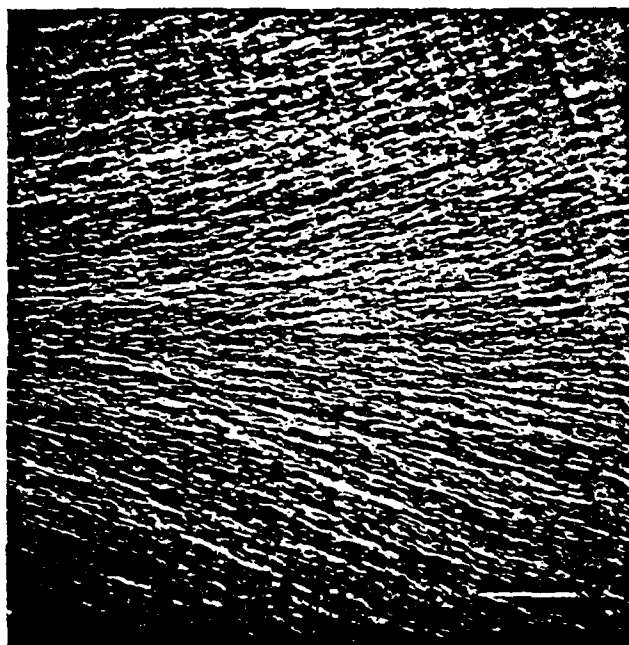


Figure 7 Fatigue striations in N66 (2.2% H₂O)
 $\Delta K = 4.5 \text{ MPa}\sqrt{\text{m}}$, Scale bar = 0.1 mm.

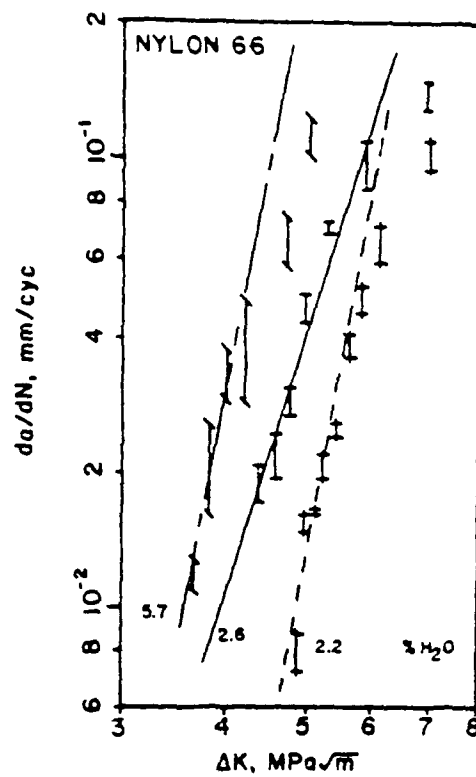
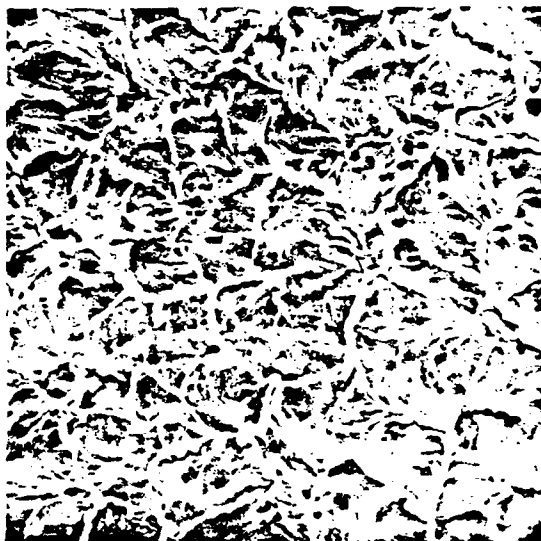
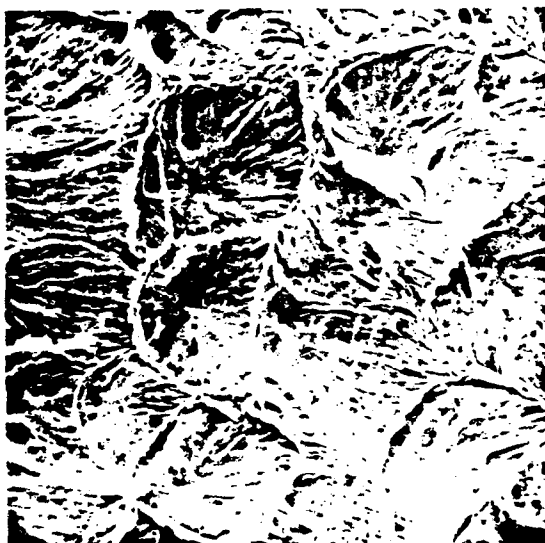


Figure 8 Correspondence between macroscopic growth increments per load cycle and measured striation spacings (scatter bands) for N66 at various moisture levels.



(a)



(b)

Figure 9 Void coalescence fracture morphology in N612.
 a) 0% H₂O, $\Delta K = 3.4 \text{ MPa}/\text{m}$, Scale bar = 0.1 mm;
 b) 3.2% H₂O, $\Delta K = 3.6 \text{ MPa}/\text{m}$, Scale bar = 0.1 mm.

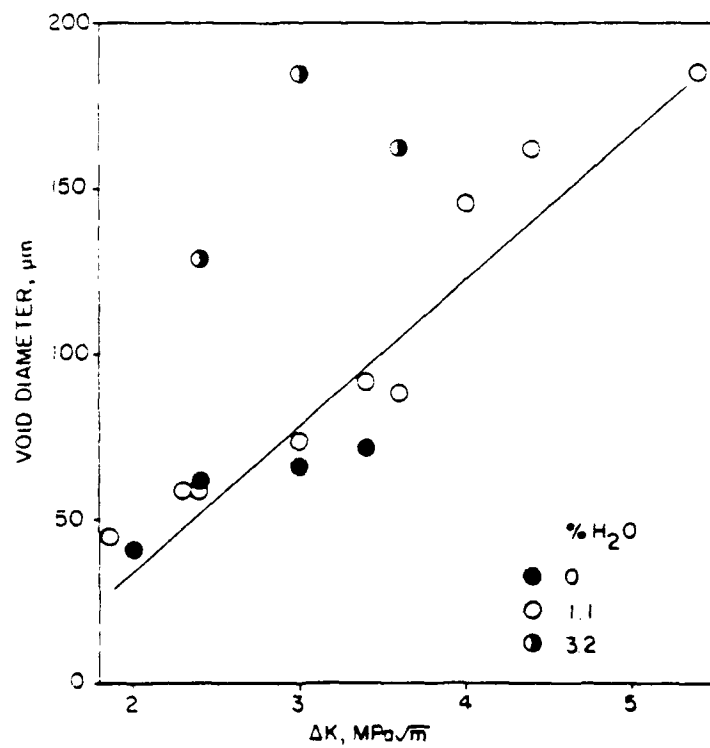


Figure 10 Dependence of void diameter on ΔK for N612 equilibrated to various levels of absorbed moisture. Note larger voids in saturated (3.2%) N612.

The microvoids in Fig. 9 seemed to radiate outward from a central depression. Closer inspection of the void centers revealed the presence of small particles within the depressions (Fig. 11a & b); these particles seemed to have a fibrillar surface texture where the polymer matrix had been drawn away. Although the nature of these particles is not certain, it is suspected that they are lubricant nodules. An EDS scan of the fracture surface showed a small concentration of aluminum in the particles. It is interesting to note that aluminum stearate is sometimes used as a lubricant in polyamides [20]. The fatigue fracture of N612 appears to be dominated by the failure of these particles and the subsequent growth and coalescence of the resulting microvoids.

4. Conclusions

1. The absorption of moisture by polyamides, particularly N66 and N6, causes dramatic changes in fatigue fracture surface appearance. In general, these variations in surface topography, both macroscopic and microscopic, reflect an increasing level of plastic deformation as water content rises.

2. The interpretation of fracture surface lineage in semi-crystalline polymers is complicated by the presence of several groupings of parallel lines produced by the fatigue fracture process. Classical fatigue striations were observed only above a certain ΔK level and in N66 and N6 specimens containing between 1.7 and 5.7% water. Their spacing agreed closely with macroscopically-determined growth rates at comparable ΔK levels. No discontinuous growth bands were identified in N66 (both MW's) N6 and N612 at all moisture levels when tests were conducted at 10 Hz. Other fracture lineage markings of undetermined origin also were seen.

3. N612 is unique among the nylons investigated in that fatigue fracture occurred by a microvoid coalescence process, regardless of moisture content. These voids seem to be nucleated by lubricant nodules of an impurity (possibly a lubricant) in the polymer.



(a)



(b)

Figure 11 Small particles at center of voids in N612.
Note fibrillar texture of particle surfaces.
a) Scale bar = 3 μm ; b) Scale bar = 10 μm .

Acknowledgements

This work was supported in part by the Office of Naval Research.
The polymers tested were supplied by E. I. duPont de Nemours & Co.,
through the courtesy of Mr. E. Flexman.

References

1. P. E. BRETZ, R. W. HERTZBERG and J. A. MANSON, J. Mater. Sci. **14** (1979) 2482.
2. P. E. BRETZ, R. W. HERTZBERG, J. A. MANSON and A. RAMIREZ, ACS Symposium Series, **127**, 1980, Paper 30.
3. P. E. BRETZ, R. W. HERTZBERG, and J. A. MANSON, The Influence of Absorbed Moisture on Fatigue Crack Propagation Behavior in Polyamides Part A: Macroscopic Response, submitted to J. Mater. Sci. 1980.
4. K. YAMADA and M. SUZUKI, Kobunshi Kagaku **30**(336) (1973) 206.
5. A. J. MCEVILY, JR., R. C. BOETTNER and T. C. JOHNSTON, in "Fatigue--An Interdisciplinary Approach," Syracuse University Press, Syracuse (1964) 95.
6. J. W. TEH and J. R. WHITE, J. Polym. Sci.-Polym. Let. Ed., **17** (1979) 737.
7. J. R. WHITE and J. W. TEH, Polymer **20** (1979) 764.
8. J. A. MANSON and R. W. HERTZBERG, CRC Rev. Macromol. Sci. **1** (1973) 433.
9. R. J. CRAWFORD and P. P. BENHAM, J. Mater. Sci. **9** (1974) 18.
10. E. H. ANDREWS and B. J. WALKER, Proc. R. Soc. London A **325** (1971) 57.
11. A. F. LAGHOUATI, Thesis, 3rd Cycle, Université de Technologie de Compiègne, 1977.
12. F. X. deCHARENTENAY, F. LAGHOUATI and J. DEWAS, 4th Inter. Conf. on Deformation, Yield, and Fracture of Polymers, Cambridge (1979) 6-1.
13. P. E. BRETZ, R. W. HERTZBERG and J. A. MANSON, Mechanisms of Fatigue Damage and Fracture in Semi-Crystalline Polymers, submitted to Polymer 1980.
14. M. D. SKIBO, R. W. HERTZBERG, J. A. MANSON and S. L. KIM, J. Mater. Sci. **12** (1977) 531.
15. R. W. HERTZBERG, M. D. SKIBO and J. A. MANSON, ASTM STP 675 (1979) 471.

16. R. W. HERTZBERG, M. D. SKIBO and J. A. MANSON, J. Mater. Sci. 13 (1978) 1038.
17. R. W. HERTZBERG and J. A. MANSON, "Fatigue in Engineering Plastics," Academic Press, New York, 1980.
18. P. E. BRETZ, R. W. HERTZBERG and J. A. MANSON, The Effect of Molecular Weight on Fatigue Crack Propagation in Nylon 66 and Polyacetal submitted to J. Appl. Polym. Sci. 1980.
19. D. Broek, Eng. Fract. Mech. 5 (1973) 55.
20. Modern Plastics Encyclopedia, McGraw-Hill, 1979-1980 p. 679.

TECHNICAL REPORT DISTRIBUTION LIST, GEN

	<u>No.</u> <u>Copies</u>		<u>No.</u> <u>Copies</u>
Office of Naval Research Attn: Code 472 800 North Quincy Street Arlington, Virginia 22217	2	U.S. Army Research Office Attn: CRD-AA-IP P.O. Box 1211 Research Triangle Park, N.C. 27709	1
ONR Branch Office Attn: Dr. George Sandoz 536 S. Clark Street Chicago, Illinois 60605	1	Naval Ocean Systems Center Attn: Mr. Joe McCartney San Diego, California 92152	1
ONR Area Office Attn: Scientific Dept. 715 Broadway New York, New York 10003	1	Naval Weapons Center Attn: Dr. A. B. Amster, Chemistry Division China Lake, California 93555	1
ONR Western Regional Office 1030 East Green Street Pasadena, California 91106	1	Naval Civil Engineering Laboratory Attn: Dr. R. W. Drisko Port Hueneme, California 93401	1
ONR Eastern/Central Regional Office Attn: Dr. L. H. Peebles Building 114, Section D 666 Summer Street Boston, Massachusetts 02210	1	Department of Physics & Chemistry Naval Postgraduate School Monterey, California 93940	1
Director, Naval Research Laboratory Attn: Code 6100 Washington, D.C. 20390	1	Dr. A. L. Slafkosky Scientific Advisor Commandant of the Marine Corps (Code RD-1) Washington, D.C. 20380	1
The Assistant Secretary of the Navy (RE&S) Department of the Navy Room 4E736, Pentagon Washington, D.C. 20350	1	Office of Naval Research Attn: Dr. Richard S. Miller 800 N. Quincy Street Arlington, Virginia 22217	1
Commander, Naval Air Systems Command Attn: Code 310C (H. Rosenwasser) Department of the Navy Washington, D.C. 20360	1	Naval Ship Research and Development Center Attn: Dr. G. Bosmajian, Applied Chemistry Division Annapolis, Maryland 21401	1
Defense Technical Information Center Building 5, Cameron Station Alexandria, Virginia 22314	12	Naval Ocean Systems Center Attn: Dr. S. Yamamoto, Marine Sciences Division San Diego, California 91232	1
Dr. Fred Saalfeld Chemistry Division, Code 6100 Naval Research Laboratory Washington, D.C. 20375	1	Mr. John Boyle Materials Branch Naval Ship Engineering Center Philadelphia, Pennsylvania 19112	1

TECHNICAL REPORT DISTRIBUTION LIST, GENNo.
Copies

Dr. Rudolph J. Marcus
Office of Naval Research
Scientific Liaison Group
American Embassy
APO San Francisco 96503

1

Mr. James Kelley
DINSRDC Code 2803
Annapolis, Maryland 21402

1

TECHNICAL REPORT DISTRIBUTION LIST, 356A

	<u>No.</u> <u>Copies</u>		<u>No.</u> <u>Copies</u>
Dr. Stephen H. Carr Department of Materials Science Northwestern University Evanston, Illinois 60201	1	Picatinny Arsenal Attn: A. M. Anzalone, Building 3401 SMUPA-FR-M-D Dover, New Jersey 07801	1
Dr. M. Broadhurst Bulk Properties Section National Bureau of Standards U.S. Department of Commerce Washington, D.C. 20234	2	Dr. J. K. Gillham Department of Chemistry Princeton University Princeton, New Jersey 08540	1
Professor G. Whitesides Department of Chemistry Massachusetts Institute of Technology Cambridge, Massachusetts 02139	1	Douglas Aircraft Co. Attn: Technical Library CI 290/36-84 AUTO-Sutton 3855 Lakewood Boulevard Long Beach, California 90846	1
Professor J. Wang Department of Chemistry University of Utah Salt Lake City, Utah 84112	1	Dr. E. Baer Department of Macromolecular Science Case Western Reserve University Cleveland, Ohio 44106	1
Dr. V. Stannett Department of Chemical Engineering North Carolina State University Raleigh, North Carolina 27607	1	Dr. K. D. Pae Department of Mechanics and Materials Science Rutgers University New Brunswick, New Jersey 08903	1
Dr. D. R. Uhlmann Department of Metallurgy and Material Science Massachusetts Institute of Technology Cambridge, Massachusetts 02139	1	NASA-Lewis Research Center Attn: Dr. T. T. Serofini, MS-49-1 21000 Brookpark Road Cleveland, Ohio 44135	1
Naval Surface Weapons Center Attn: Dr. J. M. Augl, Dr. B. Hartman White Oak Silver Spring, Maryland 20910	1	Dr. Charles H. Sherman Code TD 121 Naval Underwater Systems Center New London, Connecticut	1
Dr. G. Goodman Globe Union Incorporated 5757 North Green Bay Avenue Milwaukee, Wisconsin 53201	1	Dr. William Risen Department of Chemistry Brown University Providence, Rhode Island 02192	1
Professor Hatsuo Ishida Department of Macromolecular Science Case Western Reserve University Cleveland, Ohio 44106	1	Dr. Alan Gent Department of Physics University of Akron Akron, Ohio 44304	1

TECHNICAL REPORT DISTRIBUTION LIST, 356A

	<u>No.</u> <u>Copies</u>		<u>No.</u> <u>Copies</u>
Mr. Robert W. Jones Advanced Projects Manager Hughes Aircraft Company Mail Station D 132 Culver City, California 90230	1	Dr. T. J. Reinhart, Jr., Chief Composite and Fibrous Materials Branch Nonmetallic Materials Division Department of the Air Force Air Force Materials Laboratory (AFSC) Wright-Patterson AFB, Ohio 45433	1
Dr. C. Giori IIT Research Institute 10 West 35 Street Chicago, Illinois 60616	1	Dr. J. Lando Department of Macromolecular Science Case Western Reserve University Cleveland, Ohio 44106	1
Dr. M. Litt Department of Macromolecular Science Case Western Reserve University Cleveland, Ohio 44106	1	Dr. J. White Chemical and Metallurgical Engineering University of Tennessee Knoxville, Tennessee 37916	1
Dr. R. S. Roe Department of of Materials Science and Metallurgical Engineering University of Cincinnati Cincinnati, Ohio 45221	1	Dr. J. A. Manson Materials Research Center Lehigh University Bethlehem, Pennsylvania 18015	1
Dr. Robert E. Cohen Chemical Engineering Department Massachusetts Institute of Technology Cambridge, Massachusetts 02139	1	Dr. R. F. Helmreich Contract RD&E Dow Chemical Co. Midland, Michigan 48640	1
Dr. T. P. Conlon, Jr., Code 3622 Sandia Laboratories Sandia Corporation Albuquerque, New Mexico	1	Dr. R. S. Porter Department of Polymer Science and Engineering University of Massachusetts Amherst, Massachusetts 01002	1
Dr. Martin Kaufmann, Head Materials Research Branch, Code 4542 Naval Weapons Center China Lake, California 93555	1	Professor Garth Wilkes Department of Chemical Engineering Virginia Polytechnic Institute and State University Blacksburg, Virginia 24061	1
Professor S. Senturia Department of Electrical Engineering Massachusetts Institute of Technology Cambridge, Massachusetts 02139	1	Dr. Kurt Baum Fluorochem Inc. 6233 North Irwindale Avenue Azusa, California 91702	1
		Professor C. S. Paik Sung Department of Materials Sciences and Engineering Room 8-109 Massachusetts Institute of Technology Cambridge, Massachusetts 02139	1